EUROPEAN ORGANIZATION FOR NUCLEAR RESEARCH

CERN-EP/86-83
3 July 1986

BACKWARD SCATTERING IN $\pi^- p \to p\pi^-$, $\bar{p}p \to \pi^+\pi^-$, $K^- p \to pK^-$ AND $\bar{p}p \to p\bar{p}$ AT 8 AND 12 GeV/c

CERN[1]-Lisbon[2]-Moscow(ITEP)[3]-Neuchâtel[4]-
Paris(Coll. de France)[5]-Paris VI[6] Collaboration

T.A. Armstrong[6], M. Baubillier[6], J.C. Brient[6],
J. Dias de Deus[2], J.M. Gago[2], Yu. Galaktianov[3], J. Kahane[5],
D. Perrin[4], M. Pimenta[2], M. Sené[6], R. Sené[5],
P. Sonderegger[1], Z. Strachman[6] and R. Zitoun[6]

ABSTRACT

Data on the reactions $\pi^- p \to p\pi^-$, $pp \to \pi^+\pi^-$, $K^- p \to pK^-$ and $\bar{p}p \to p\bar{p}$ at 8 and 12 GeV/c are presented. Our results agree with Line Reversal Symmetry (between $\pi^- p \to p\pi^-$ and $\bar{p}p \to \pi^+\pi^-$), Regge pole behaviour for non exotic reactions ($\pi^- p \to p\pi^-$, $\bar{p}p \to \pi^+\pi^-$), and universal behaviour for exotic reactions ($\bar{p}p \to p\bar{p}$, $K^- p \to pK^-$) with $d\sigma/du|_{u=0} \sim s^{-10}$ excluding the existence of a "glory" mechanism in pp elastic backward scattering in our energy range.

(To be submitted to Nuclear Physics B)

---

1 CERN, Geneva, Switzerland.
2 INIC, Instituto Nacional de Investigaçao Cientifica, Lisbon, Portugal.
3 Institute of Theoretical and Experimental Physics, Moscow.
4 Institut de Physique, Université de Neuchâtel, Switzerland.
5 Lab. de Physique Corpusculaire, Collège de France, Paris, France.
6 LPNHE, Université Pierre et Marie Curie, Paris, France.

0034P/JMG/sm

1. INTRODUCTION

Backward scattering is an interesting and open problem. In reactions where the quantum numbers required for the exchange in the u channel correspond to well established particles or resonances there is a peak in the differential cross-section near u = 0 with a weak energy dependence ($\sim s^{-2}$ to s^{-3}). This behaviour has been explained in Regge pole models by the exchange of Regge trajectories. On the contrary, when no particles or resonances can be exchanged in the u channel (exotic reactions), no backward peak and a strong energy dependence of the differential cross-section at u = 0 is normally observed. However, twelve years ago [1], backward peaks were reported in $K^-p \to pK^-$ and in $\bar{p}p \to p\bar{p}$ at an incident laboratory momentum of 5 GeV/c and the measured value of the differential cross-section at $u \simeq 0$ was compatible with the strong energy dependence ($\sim s^{-10}$) established in a lower momentum range by previous experiments [2,3]. We note that a similar strong energy dependence is observed in the large angle region (60°-120°).

The main purpose of the present experiment was to measure $\bar{p}p$ backward elastic scattering at energies higher than 5 GeV/c in order to verify whether the mechanism responsible for the observed backward peaks at 5 GeV/c implied any change from the strong energy dependence to a weaker one in the differential cross-section at u = 0 or not. Such a behaviour was suggested in analogy with the classical optical phenomenon known as glory scattering. Other two-body reactions were also studied in the backward region.

We present here the results obtained for exotic ($K^-p \to pK^-$, $\bar{p}p \to p\bar{p}$) and non exotic ($\pi^-p \to p\pi^-$, $pp \to \pi^+\pi^-$) reactions in the backward region at 8 and 12 GeV/c.

A fair agreement between our results in $\pi^-p \to p\pi^-$ and those published for the same reaction and range of energy [4-7] is reported.

$\bar{p}p \to \pi^+\pi^-$ and $\pi^-p \to p\pi^-$ data were measured, at 12 GeV/c, under nearly identical conditions. Systematic errors in the comparison of these two reactions were, therefore, minimized. These two reactions have the same u channel exchange quantum numbers. The prediction of Line Reversal Symmetry for the ratio of the total backward cross-sections of these two reactions

was confirmed. Earlier simultaneous measurements had established this symmetry for incident momenta lower than 6 GeV/c [1,8].

In $K^- p \to pK^-$ and $\bar{p}p \to p\bar{p}$ upper limits in backward cross-sections at 8 and 12 GeV/c are reported. The limit in $\bar{p}p \to p\bar{p}$ rules out the possibility of a weak energy dependence associated with the previously observed backward peak at 5 GeV/c.

In Section 2 of this paper we discuss the apparatus and the trigger, in Section 3 the data analysis and in Section 4 we present the experimental results. The main conclusions are outlined in Section 5.

2. EXPERIMENTAL SET-UP AND TRIGGER

The experiment was performed at the CERN Omega Spectrometer (Fig. 1) exposed to an unseparated negative hadron beam. Pions were the main components of the beam (~ 97%). In order to achieve good sensitivities in $\bar{p}$ we were forced to work at the highest possible intensity ($2-3 \times 10^7$ particles per burst). The momentum of the beam was measured, with a non interaction trigger, in the Omega Spectrometer. Its standard deviation was found to be ~ 50 MeV/c. In the beam line there were three Cerenkov counters: two threshold Cerenkov (TC1 and TC2) and one differential Cerenkov counter (CEDAR). At 8 GeV/c, beam identification was obtained using TC1 and TC2, and at 12 GeV/c, using TC2 and CEDAR. Inside the 1.7 T vertical magnetic field 69 MWPC planes measured the charged particles momenta: 37 in the forward region and 16 at each side of the 60 cm hydrogen target. In addition, two drift chambers, 4.5 and 5.7 m downstream of the target, allowed the measurement of forward tracks with an accuracy $\Delta p/p < 1\%$. Fast protons were identified by one threshold Cerenkov counter (C1). A second threshold Cerenkov counter (C2) established, over a smaller acceptance region, that the efficiency in this identification was greater than 99%. A 24-channel cylindrical hodoscope (Barrel) surrounded the target. In each Barrel scintillator the energy loss was measured which allowed the separation between π^- and p for momenta less than 600 MeV/c.

A three level trigger looked for protons with momentum similar to the momentum of the incoming beam. In the first level, beam definition was

established by the coincidence of four small scintillation counters and all the electrons and the majority of pions were rejected by a veto signal from the beam Cerenkov TC2. The second and the third trigger levels were built in MBNIM logic [9] and gave a first measurement of the fast proton momentum. A correlation between hits in hodoscopes H1 and H2, was required in the second level trigger. The third level trigger required a finer correlation between H2 and a y plane of one of the last wire chambers.

3. EVENT RECONSTRUCTION AND DATA ANALYSIS

The purpose of the analysis was to select two body reaction candidates among all triggers. In order to obtain the best cross-section upper limits we had to resort to non standard procedures which are summarized hereafter. A more detailed description is given in Ref. 10.

The normal TRIDENT procedure [11] was used to reconstruct the fast and the slow particle trajectories leading to a straightforward kinematical fit. The efficiency of this procedure was however found to be insufficient to get meaningful results, mainly because of the small number of planes, the moderate efficiency and the considerable background in the side chambers. The sample of $\pi^- p \to p\pi^-$ thus obtained was however used to check the performance of the alternative procedures outlined hereafter.

A missing mass analysis, based only on the information of the fast particle and on beam parameters measured in separated beam runs, was good enough to identify the elastic peak in $\pi^- p \to pX$ ($\delta MM^2 \simeq 0.2$ GeV^2/c^4). However in $K^- p \to pX$ and in $\bar{p}p \to pX$ a small inefficiency in the beam identification gave rise to an important and prohibitive background from $\pi^- p \to pX$.

A hybrid strategy was therefore adopted: we performed a missing mass analysis but we reduced the background by requiring a majority of MWPC planes to exhibit signals in the vicinity of the slow particle trajectory as predicted from a two body reaction kinematics. A check on pulse height of the intersected Barrel counter was also made.

The fast particle trajectory was reconstructed by TRIDENT from forward MWPCs and drift digitizations. Only fast tracks with reconstructed space points in drift chambers were accepted. The distance between the extrapolated fast particle trajectory and the nominal beam at the closest approach point within the target was required to be comparable with measured beam parameters.

Two body kinematical constraints allowed the prediction of the possible slow particle paths as a function of the vertex position within the target. A systematic search for recoil particle digitizations in side and/or forward MWPC chambers, starting at the nearest planes from the target, was done. Whenever a digitization was found a reduced window was predicted for the next planes from the possible paths and the beam dispersion.

Pulse heights in the intersected Barrel counter, corrected for scintillator attenuation along the scintillator were then compared with calculated energy deposition using Bethe-Bloch formula. The attenuation length and the corresponding dE/dx calibration and an average efficiency (90%) of each Barrel counter was determined using πp forward and backward elastic events reconstructed by TRIDENT.

Events with a good missing mas (within a 3 standard deviation interval), digitizations in more than a half of the intersected MWPC planes and a fair agreement between calculated energy deposition and Barrel pulse heights, were considered as candidates to two body reactions. This criterion has a global acceptance more than two times higher than complete four constraints kinematic fits. For the case of $\bar{p}p \to p\bar{p}$ our procedure is strictly limited to $u > 0.05$ GeV/c^2 where the recoil p reaches side chambers. In the following we used the reported 5 GeV/c u slope [$<|u|> = 0.25$ (GeV/c)^2] to account for the small unseen region.

The geometrical acceptance of the apparatus, at each incident beam and momentum, was determined by a Monte Carlo program. Events were generated in the hydrogen target (using measured beam parameters) and the scattered particles were followed through the spectrometer. Trigger conditions were imposed, as well as its measured inefficiencies for forward particles at certain angles.

We present in Table 1 the calculated acceptances for the several energies and reactions studied.

4. EXPERIMENTAL RESULTS AND DISCUSSION

The cross-sections measured in this experiment are presented in Table 1. The errors quoted in this table are one standard deviation and include statistical and systematic errors.

4.1 $\pi^- p$ backward elastic scattering

The differential cross-section $d\sigma/du$ for $u > -1$ GeV$^2/c^2$ at 8 and 12 GeV/c is shown in Fig. 2. We have fitted the data to the form $d\sigma/du = A \exp(Bu)$ and the values found for the parameters A and B are also presented in Table 1.

A fair agreement is observed between our values and those from other experiments [4-7]. As previously noticed [12] a simple baryon exchange Regge pole model, using only $\Delta\gamma$ trajectory, can explain the data.

4.2 The annihilation reaction $\bar{p}p \to \pi^+\pi^-$

The backward cross-sections for incident momentum at and above 5 GeV/c are represented in Fig. 3.

Our value at 12 GeV/c, when compared with those obtained at 5 and 6 GeV/c [1,8], is compatible with a weak energy dependence ($\sim p_{lab}^{-2.3 \pm 0.4}$) similar to the one observed in $\pi^- p \to p\pi^-$ [1,12]. The value reported at 6.2 GeV/c [13] is in contradiction with this dependence.

The ratio between our measured cross-sections in $pp \to \pi^+\pi^-$ and $\pi^- p \to p\pi^-$ at the same centre of mass energy, $\sqrt{s} = 4.93$ GeV/c, obtained by extrapolating the $\pi^- p \to p\pi^-$ result over a small interval using s^{-2} scaling laws, is 0.45 ± 0.20. This ratio agrees with Line Reversal Symmetry predictions (0.55 [14], 0.58 [15]) which include spin and phase-space differences.

4.3 $\bar{p}p$ backward elastic scattering

In the backward region ($u > -1.5$ GeV$^2/c^2$) we have 5 events at 8 GeV/c and 0 events at 12 GeV/c. However, at 8 GeV/c, the background due to inefficiencies in the beam identification is too large to provide a significant signal to background ratio. We can thus only give upper limits for backward cross-sections. In fact we estimate the background as 3.8 ± 1.0 and 1.6 ± 0.3 events at 8 and 12 GeV/c.

The upper limits in the backward cross-section presented in Table 1, for this reaction, were then calculated considering an upper limit for the signal of 1.2 ± 2.5 and 0 ± 1 events at 8 and 12 GeV/c, respectively.

In Fig. 4 we present the differential cross-section $d\sigma/dt$ outside the forward peak for several incident momenta. Our data at 8 and 12 GeV/c do not exclude the possibility of backward peaks as the ones observed at 5 and 6.2 GeV/c.

In Fig. 5 we present the differential cross-section $d\sigma/du$ at $u = 0$ as a function of the logarithm of the square of the centre of mass energy (s). Our measured points, as well as the data points at 3.66 and 6.2 GeV/c were obtained by assuming an exponential parametrization of the backward peak with a slope of 4 $(GeV/c)^{-2}$, since the measurements only give limits on integrated cross-sections in the backward region. The energy dependence of the differential cross-section at $u = 0$ is generally parametrized as $d\sigma/du|_{u=0} \propto s^{-\alpha}$. The value of α for incident momenta equal or higher than 5 GeV/c is now established to be greater than 8.0 ± 3.4. This value must be compared with a previous fit between 2 and 5 GeV/c of incident momenta which indicated $\alpha = 9.5$ [1].

4.4 $\underline{K^- p}$ backward elastic scattering

In the backward region ($u > -1.5$ GeV^2/c^2) we have 4 events at 8 GeV/c and 0 events at 12 GeV/c but the estimated background (2.0 ± 1.5 and 1.4 ± 1.6 events at 8 and 12 GeV/c) is of the same order. We present then only upper limits for backward cross-sections. The values presented in Table 1 were calculated considering an upper limit for the signal of 2.0 ± 2.5 and 0 ± 1 events at 8 and 12 GeV/c.

These results cannot establish whether the prediction [16] of a change from the strong energy dependence ($\sim s^{-10}$) on the differential cross-section at $u = 0$ to a weaker dependence regime ($\sim s^{-3}$), is true or not.

5. CONCLUSIONS

We have measured backward cross-sections in exotic ($K^- p \to pK^-$, $\bar{p}p \to p\bar{p}$) and non exotic ($\pi^- p \to p\pi^-$, $\bar{p}p \to \pi^+\pi^-$) reactions at 8 and 12 GeV/c.

In non exotic reactions we confirmed the weak energy dependence regime of the differential cross-sections at u = 0. This behaviour is described for the studied reactions by a Regge pole model with the exchange of a single Δ trajectory.

In exotic $\bar{p}p \to p\bar{p}$ we established that the strong energy dependence regime previously observed in the differential cross-section at u = 0 is still valid at 12 GeV/c. In $K^-p \to pK^-$ the same regime is compatible with our data.

In the framework of optical models extended to the backward region (glory scattering) a weak energy dependence regime for the differential cross-section at u = 0 was predicted [17]. Our data shows that, in the reaction $\bar{p}p \to p\bar{p}$, this mechanism is <u>not</u> seen at energies up to 12 GeV/c therefore that mechanism cannot be responsible for the reported backward peak at 5 GeV/c.

Regge pole models for the backward region in exotic reactions [16,18] are strongly dependent on the particular u channel exchange and, therefore, give no explanation for the universal behaviour of those reactions, which is suggested by all experimental data.

REFERENCES

[1] A. Eide et al., Nucl. Phys. B 60 (1973) 173.

[2] D.L. Parker et al., Nucl. Phys. B 32 (1971) 29.

[3] W.M. Katz et al., Phys. Rev. Lett. 19 (1967) 265.

[4] A. Yacholkowski et al., Nucl. Phys. B 126 (1977) 1.

[5] W.F. Baker et al., Nucl. Phys. B 25 (1971) 385.

[6] D.P. Owen et al., Phys. Rev. 181 (1969) 1794.

[7] E.W. Anderson et al., Phys. Rev. Lett. 20 (1968) 1529.

[8] N. Scharfman et al., Phys. Rev. Lett. 40 (1978) 681.

[9] F. Bourgeois, MBNIM User's Guide, CERN, Internal Report.

[10] M. Pimenta, Ph.D. Thesis, Lisbon University (1986).

[11] J.C. Lassalle et al., CERN-DD/EE/79-2.

[12] W.F. Baker et al., Phys. Rev. D 27 (1983) 1999.

[13] T. Buram et al., Nucl. Phys. B 116 (1976) 51.

[14] D. Jackson, Proc. Int. Conf. on Duality and Symmetry in Hadron Physics (Weizman, 1971), 1.

[15] V. Barger and D. Cline, Phys. Lett. 25B (1967) 415.

[16] C. Michael, Phys. Lett. 29B (1969) 230.

[17] J. Dias de Deus and M. Pimenta, IFM 10/85, preprint.

[18] P. Kroll, Wuppertal University, 84-13 preprint.

[19] P. Billoir, thèse Doctorat d'Etat, LPCT 8301.

[20] T. Buram et al., Nucl. Phys. B 97 (1975) 11.

[211 D.L. Parker et al., Nucl. Phys. B 32 (1971) 29.

[22] W.M. Katz et al., Phys. Rev. Lett. 19 (1967) 265.

Table 1

Acceptance, sensitivity and cross-sections in the backward region ($u > -1.5$ GeV$^2/c^2$) for the reactions and energies studies. The differential cross-sections are parametrized as $d\sigma/du|_{u\simeq 0} = A \exp(Bu)$. The errors and upper limits quoted in this table are one standard deviation and include statistical and systematic errors.

Reaction momentum	Acceptance	Sensitivity (nb/ev)	Integrated cross-section (nb)	A differential cross-section at u = 0 [nb (GeV/c)$^{-2}$]	B slope of the differential cross-section at u ≃ 0 (GeV/c)$^{-2}$
$\pi^- p \to p\pi^-$ 8 GeV/c	0.16	0.78	1080 ± 175	3540 ± 650	3.86 ± 0.25
$\pi^- p \to p\pi^-$ 12 GeV/c	0.14	0.12	240 ± 35	750 ± 120	3.53 ± 0.20
$\bar{p}p \to \pi^+\pi^-$ 12 GeV/c	0.09	5.9	100 ± 30	360 ± 108	3.53 *)
$\bar{p}p \to p\bar{p}$ 8 GeV	0.19	2.8	< 12.5	< 50	4 *)
$\bar{p}p \to p\bar{p}$ 12 GeV/c	0.18	1.2	< 1.5	< 6	4 *)
$K^- p \to pK^-$ 8 GeV/c	0.19	35	< 156	< 503	3.2 *)
$K^- p \to pk^-$ 12 GeV/c	0.17	2.4	< 2.4	< 8	3.2 *)

*) Values for the slope B of the differential cross-section were taken for $\bar{p}p \to \pi^+\pi^-$ from our measured value in $\pi^- p \to p\pi^-$ and for exotic reactions from Ref. [1]. The values of B reported in the table were used for the determination of the differential cross-section at u = 0 (A).

Figure captions

Fig. 1 : The experimental layout of the Omega Prime Spectrometer.

Fig. 2 : Differential cross-section near u = 0 in $\pi^- p \to p\pi^-$ at 8 and 12 GeV/c, the lines represent our best fits to the data.

Fig. 3 : Integrated cross-section in the backward region for $\bar{p}p \to \pi^+\pi^-$ at 12 GeV/c compared with data from previous experiments at lower energies [1,8,13].

Fig. 4 : Differential cross-section $d\sigma/dt$ outside forward peaks in $\bar{p}p \to \bar{p}p$ at several energies. Data points from previous experiments were taken from Refs. [1,19,20].

Fig. 5 : Differential cross-section $d\sigma/du$ at u = 0 as a function of the energy of the centre of mass energy. Data points from previous experiments were taken from Refs. [1,20-22].

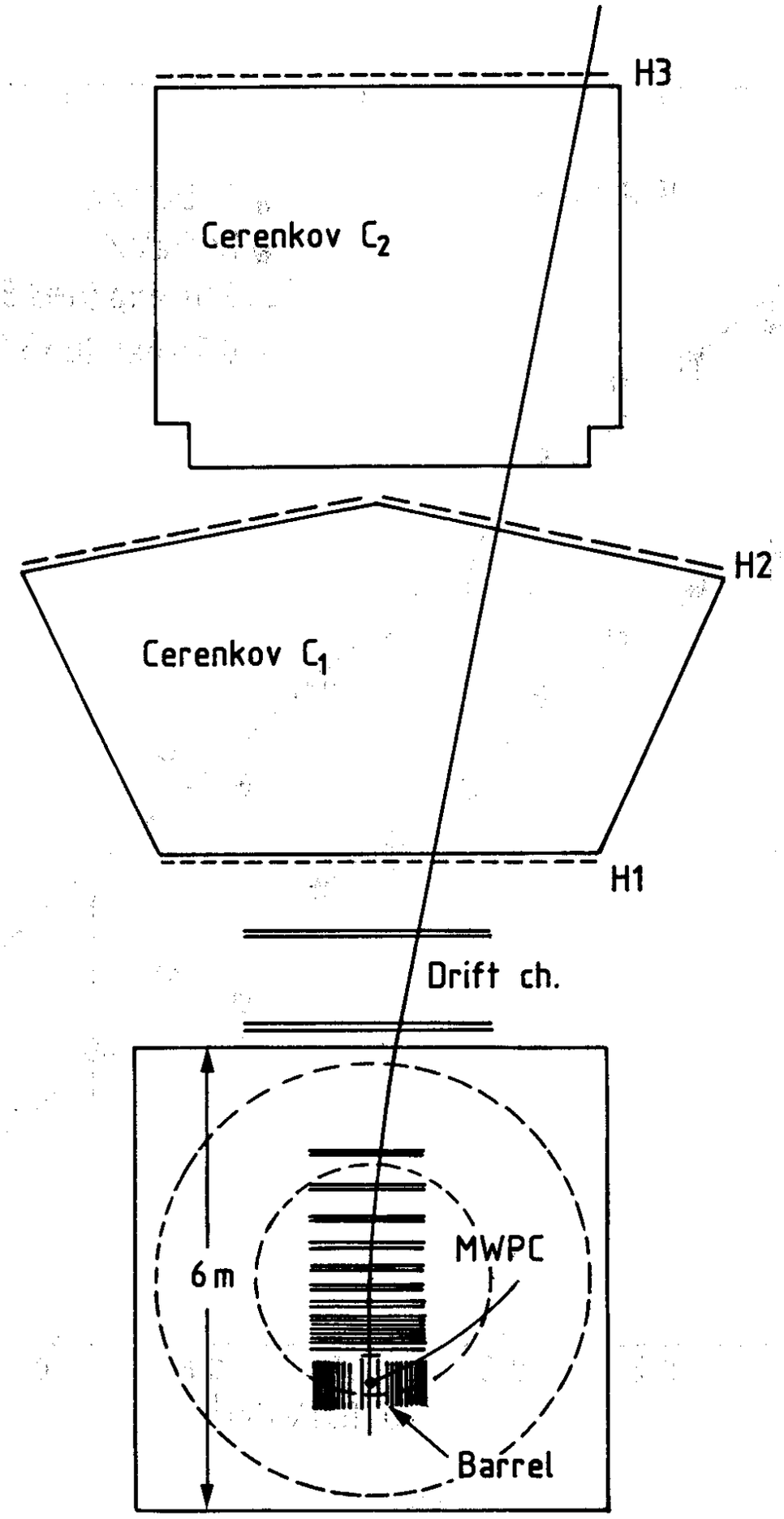

Fig. 1

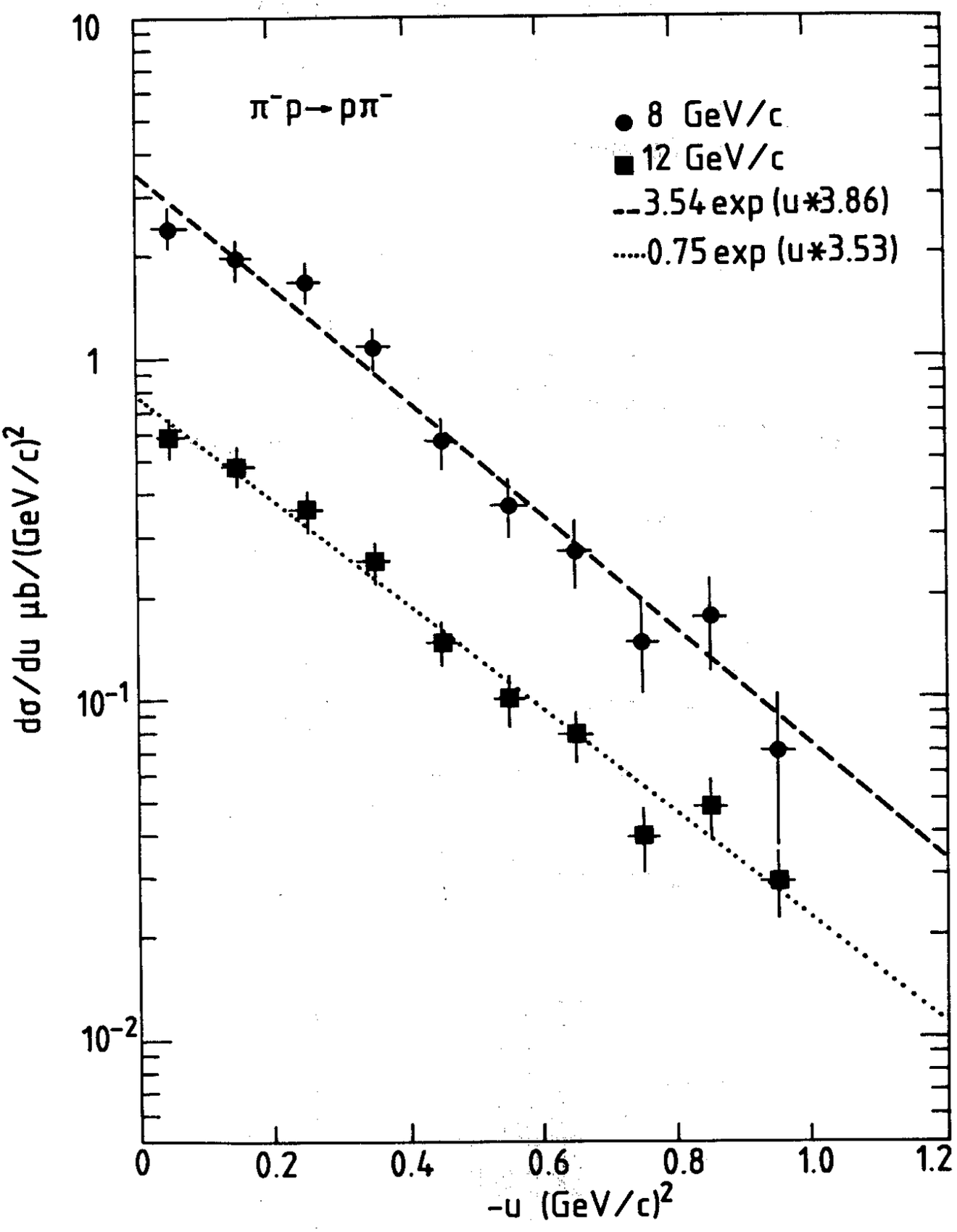
10
1
10^{-1}
10^{-2}
$\pi^- p \rightarrow p\pi^-$
8 GeV/c
12 GeV/c
--3.54 exp (u*3.86)
.....0.75 exp (u*3.53)
$d\sigma/du$ μb/(GeV/c)^2
0
0.2
0.4
0.6
0.8
1.0
1.2
$-u$ (GeV/c)^2

Fig. 2

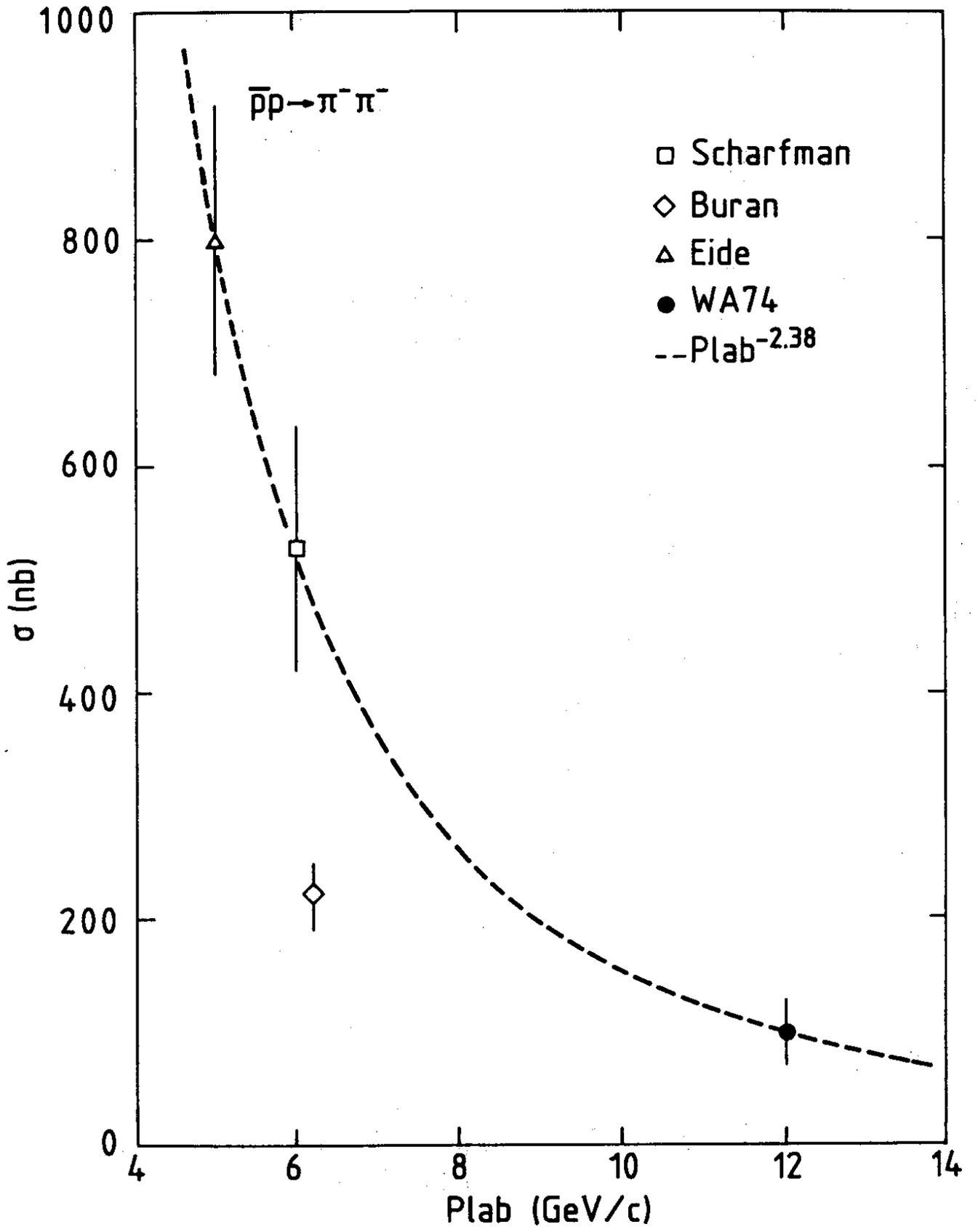
1000
800
600
400
200
0
σ (nb)
4
6
8
10
12
14
Plab (GeV/c)
p̄p→π⁻π⁻
Scharfman
Buran
Eide
WA74
--Plab^-2.38

Fig. 3

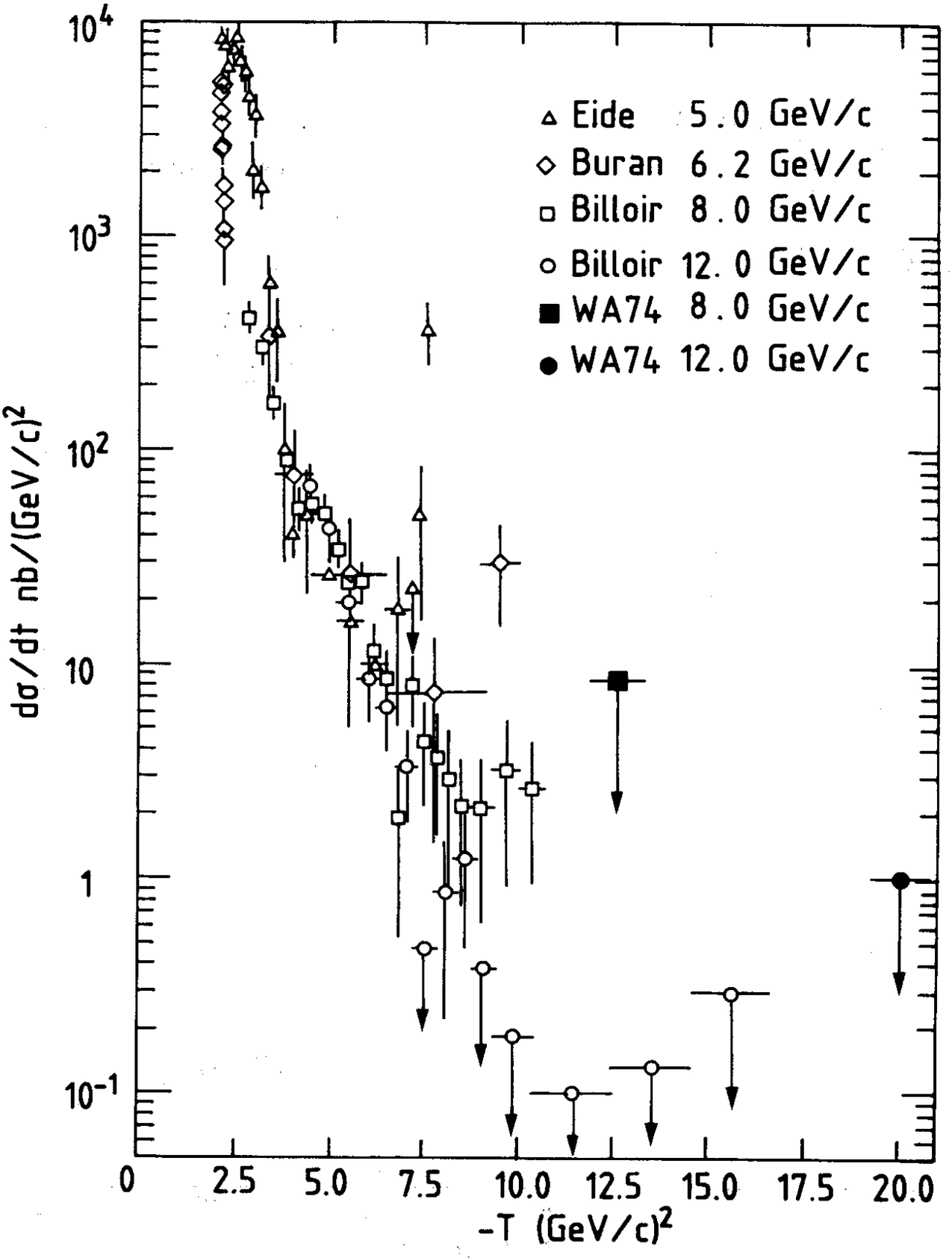
Eide 5.0 GeV/c
Buran 6.2 GeV/c
Billoir 8.0 GeV/c
Billoir 12.0 GeV/c
WA74 8.0 GeV/c
WA74 12.0 GeV/c
dσ/dt nb/(GeV/c)²
-T (GeV/c)²
10⁴
10³
10²
10
1
10⁻¹
0
2.5
5.0
7.5
10.0
12.5
15.0
17.5
20.0

Fig. 4

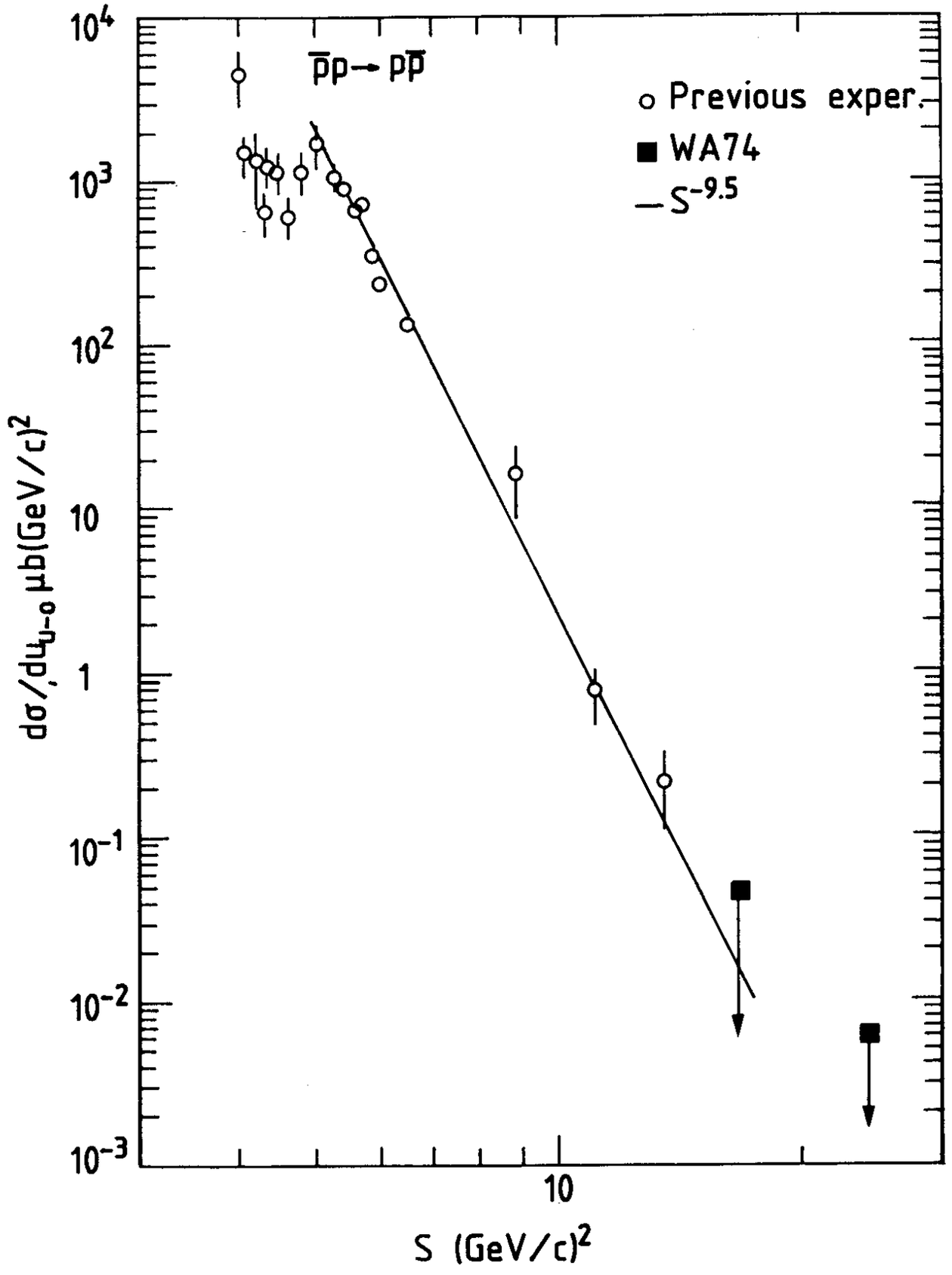
$\bar{p}p \rightarrow p\bar{p}$
o Previous exper.
■ WA74
$-S^{-9.5}$
10^4
10^3
10^2
10
1
10^{-1}
10^{-2}
10^{-3}
$d\sigma/du_{u=0}\ \mu b(GeV/c)^2$
10
$S\ (GeV/c)^2$

Fig. 5